Poly(lactic acid)-Modified Films for Food Packaging Application: Physical, Mechanical, and Barrier Behavior

Valentina Siracusa,[1] Ignazio Blanco,[1] Santina Romani,[2] Urtzula Tylewicz,[2] Pietro Rocculi,[2] Marco Dalla Rosa[2]

[1]*Department of Industrial and Mechanical Engineering (DIIM), Engineering Faculty, University of Catania, 95125 Catania (CT), Italy*
[2]*Department of Food Science, Alma Mater Studiorum, University of Bologna, Piazza Goidanich 60, 47521 Cesena (FC), Italy*

Received 1 June 2011; accepted 17 January 2012
DOI 10.1002/app.36829
Published online in Wiley Online Library (wileyonlinelibrary.com).

ABSTRACT: Poly(lactic acid) (PLA) is now a very attractive polymer for food packaging application because in addition of being thermoplastic, biodegradable, compostable, and produced from renewable resources, it shows same behavior in mechanical, thermal, and barrier properties comparable to the most used synthetic polymers like polystyrene and poly(ethylene terephthalate). In this work, we take into consideration four commercial PLA films, natural- and surface-modified, to make a correlation between mechanical, thermal, and barrier properties due to the surface modification, to well understand whether PLA is adapt to packaging application, especially in the food field. Films were studied by tensile testing, simultaneous differential thermal analysis/thermogravimetry, differential scanning calorimetry, permeation to carbon dioxide and oxygen at different temperature (7 and 23°C) and FTIR spectroscopic analysis.
 J Appl Polym Sci 000: 000–000, 2012

Key words: mechanical properties; thermal properties; biopolymers; poly(lactic acid) (PLA); food packaging

INTRODUCTION

For a long time, polymers have supplied most of common packaging materials because they present several desired features like softness, lightness, and transparency. Until now petrochemical-based plastics such as poly(ethylene terephthalate) (PET), poly(vinyl chloride) (PVC), polyethylene (PE), low-density polyethylene (LDPE), high-density polyethylene (HDPE), polypropylene (PP), polystyrene (PS), and polyamide (PA) have been increasingly used as packaging materials. This is because of their large availability at relatively low cost and because of their good mechanical performance such as tensile and tears strength, good barrier to oxygen, carbon dioxide, anhydride, and aromatic compound, heat sealability, and so on. However, an increased use of synthetic packaging films has led to serious ecological problems due to their total non-biodegradability. Although their complete replacement with eco-friendly packaging films is just impossible to achieve at least, for specific applications like food packaging, the use of bioplastics should be the future.[1] Plastic packaging materials are also often contaminated by foodstuff and biological substance, so recycling these materials is impracticable and most of the time not convenient economically. As a consequence several thousands of tons of goods, made on plastic materials, are land filled, increasing every year the problem of municipal waste disposal.[2] The growing environmental awareness imposes to packaging films and process both user-friendly and eco-friendly attributes. As a consequence, biodegradability is not only a functional requirement but also an important environmental attribute, so it is becoming increasingly important to utilize alternative raw materials to produce packaging materials.

Bioplastics, like plastics, present a large spectrum of application such as collection bags for compost, agricultural foils, horticultures, nursery products, toys, fibers, textiles, etc. Other fields, such as packaging and technical application, are gaining importance but to manufacture a product using a 100% renewable resources is neither impossible in the early future and the tendency is to utilize the possible highest proportion of renewable resources. Until now bioplastics contain more than 50% weight of renewable resources.[1]

The performance expected from bioplastics materials used in food packaging application is containing the food, protecting it from the environment contamination and maintaining food quality for all the storage time.[3] It is obvious that to perform these

Correspondence to: V. Siracusa (vsiracus@dmfci.unict.it).

functions is important to control and modify their barrier properties, which consequently depend on the internal architecture of the polymer (stereochemical make-up of the backbone) and on the molecular mass. The possibility to control the stereochemical architecture of a material gives the possibility to control the degree of crystallinity, the mechanical properties, and the processing temperature which is correlated to the thermal behavior. Further, stereo-chemical composition, molecular weight, and crystallinity control also the degradation behavior. Poly(lactic acid) (PLA) shows the advantage to easy change and tailors their physical, mechanical properties by simply changing the chemical composition (amount of D- and L-isomer) and the processing conditions.[4]

Concerning the barrier properties, to enhance their value going from a medium to a high gas barrier polymer, a surface polymer modification can be taken into consideration. It can be achieved, for example, by the ultraviolet (UV) light blockers, which are often used in clear or tinted packaging to protect food and beverage products from UV light degradation coming from sunlight or in-store fluorescent lighting. UV light can degrade the color, flavor, and nutritional value of particularly susceptible food product like fruit juice, tea, and sport drink, so surface modification makes the polymer not only less permeable to the gas but more stable.

When the surface polymer modification is achieved with a coating of SiO_x, the peculiar properties of the polymer material such as tenacity, flexibility, transparency, processability, low cost, and good adhesion to substrate, enter in synergy with those of the inorganic component such as toughness, flame retardancy, chemical, and thermal stability, low cost and, above all gas barrier property. In literature, several data on the use of SiO_x and other ceramics as coating to improve the gas barrier properties of polymeric materials are reported, but most of the information are referred to synthetic polymers like PET, PP, and PET/PE copolymer.[5–7]

The selection of the correct packaging material is crucial, as the packaging material needs to be flexible enough to withstand compression forces while maintaining physical integrity and suitable barrier properties to gas, water vapor, and aromas.[8]

Among the biodegradable material studied until now in the literature,[9] PLA has received increasing attention due to their natural biodegradability which made it interesting for biomedical, pharmaceutical, and food applications. Further, as reported by Conn et al.,[10] PLA is safe and generally recognized as safe for its use in contact with food, approved from the Food and Drug Administration.

Of course, like for the other plastics, final properties and material use depend on their chemical–physical, thermal, mechanical, and barrier properties that can be modulated for each specific application by changing the polymer structure (crystalline/amorphous ratio, molecular mass, different proportion of L, D, or *meso*-lactide). This results in a PLA polymer with a wide range of hardness and stiffness, glass transition temperature (T_g), melting temperature (T_m), and barrier value.

As PLA can offer several opportunities in the food packaging field, it need to better understand and describe its characteristics examining the physical, mechanical, and barrier properties. The purpose of the present work is just to investigate the selected properties on four PLA films, natural- and surface-modified, to improve their barrier performance, to achieve information about the suitability of this material to be used for food service application. The films were achieved from industrial source.

EXPERIMENTAL

Materials

Four PLA films were studied as received, without any special preliminary treatments. The specific surface treatments are under industrial secrets so is not possible to give a detailed description of the treatment methods used. All compounds are made of a PLA film on a polymer substrate: one was a natural PLA film while the other three were subject by the supplier to superficial treatments in order to change their barrier properties.

The films were identified as following:

- **PLA1**: natural PLA film
- **PLA2**: PLA with SiO_x coating
- **PLA3**: PLA with anti-UV coating
- **PLA4**: PLA varnished

Instruments

Tensile test

Mechanical tests in tensile mode were performed with a Texture Analyser TA.HDi type, with a Tensile Grip (A/TG) accessory, in a conditioned room at 23°C, using the following operative conditions: Test mode: measure force in tension; pretest speed: 5.00 mm/s; test speed: 1.5 mm s^{-1}; distance: 30%; load cell: 50 kg; temperature: 23°C. Tests were conducted on samples cut both in the extrusion machine direction (MD) and in the extrusion cross direction (CD), as showed in Figure 1.

The results are an average of 30 experimental tests run on 30 different samples for each PLA film in MD and CD cut direction. Tests were performed according to the ASTM D-882-09 Standard Test

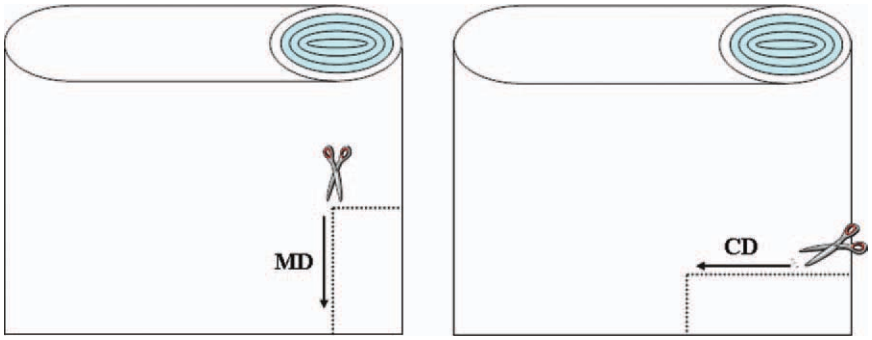

Figure 1 Sample cut mode for the PLA films coil. [Color figure can be viewed in the online issue, which is available at wileyonlinelibrary.com.]

Method for Tensile Properties of Thin Plastic Sheeting norm.

For each test, the parameters obtained from the curves were:

- the maximum value expressed in N mm^{-2}, reached by the force, which represents the maximum material resistance showed to tensile extension (tensile strength);
- the distance, in %, calculated on the *x*-axis from the zero point to the first vertical drop of the curve (point of failure). It represents the fracture percentage of elongation, i.e., the capacity of the material to stretch without breaking;
- the underlying area to the curve expressed as N mm^{-2} %, representing the material toughness.

DSC measurements

Calorimetric measurements were performed by a Perkin-Elmer type Pyris DSC-6 Instrument, equipped with a liquid sub-ambient accessory and calibrated with high-purity standards such as indium and tin. The external block temperature control was set at −30°C. Polymer films were cut into small pieces of 2 mm^2 and placed in a 40-μL sealed aluminum crucibles. Samples of the average weight of 5–7 mg have been prepared. In order to avoid film contamination, special care was taken during handling. All tests were run under pure nitrogen flow (0.02 L min^{-1}). An empty aluminum crucible has been used as reference. Differential scanning calorimetry (DSC) measurements were performed in triplicate. The heat program, registration data, and their subsequent processing are controlled by a PC connected to the calorimeter.

After an isotherm of 5 min at 10°C, weighed samples were heated to 180°C, about 35°C above fusion temperature, at a rate of 10°C min^{-1} (first scan) and then, after a further isotherm of 3 min at 180°C, were quenched to 10°C at a rate of 40°C min^{-1}. Finally, after an isotherm at this temperature for 3 min, they were reheated from 10°C to a temperature well above the fusion temperature of the sample, at a heating rate of 10°C min^{-1} (second scan).

The glass-transition temperature (T_g) was taken as the midpoint of the heat capacity increment Δc_p associated with the glass–rubber transition. The melting temperature T_m was determined as the peak value of the endothermal phenomena in the DSC curve while the crystallization temperature T_c was determined as the peak value of the isothermal phenomena in the DSC curve. The specific heat increment Δc_p, associated with the glass transition of the amorphous phase, was calculated from the vertical distance between the two extrapolated baselines at the glass transition temperature. The heat of fusion ΔH_m of the crystal phase was calculated from the area of the DSC endothermic peak. Repeated measurements on each sample showed good reproducibility.

T_g, T_c, and T_m values are well reproducible from the second scan, while those relating to the first scan are affected by thermal and mechanical history to which the samples were subjected.

Thermal analysis

A Shimadzu DTG-60 simultaneous differential thermal analysis/thermogravimetry (DTA-TG) apparatus was used for DTA and TG. Temperature, heat flow, and weight calibration were performed following the procedure reported in the instruction manual,[11] using indium (NIST SRM 2232), tin (NIST SRM 2220), and zinc (NIST SRM 2221a) as standard materials for temperature; indium (NIST SRM 2232) standard material for heat flow and a set of exactly weighed samples supplies by Shimadzu for weight. All calibrations were repeated every two weeks.

Scannings were carried out under flowing nitrogen (0.02 L min^{-1}) and in a static air atmosphere, in dynamic heating conditions, in the temperature range from 35°C to 700°C, at heating rate of 10°C

min^{-1}. Samples of about 10×10^{-3} g were cut into small pieces of 2 mm^2, placed in a platinum capsule of 40 μL, and used for experiments. In order to avoid contamination of the film, special care was taken during handling. For thermogravimetric analysis, sample weights as a function of temperature were monitored and recorded by a PC connected with the DTG-60 apparatus and, at the end of each experiment, data were used to plot the percentage of undegraded sample $(1 - D)\%$ as a function of temperature, where $D = (W_o - W)/W_o$, with W_o and W the sample weight at the starting point and during scanning, respectively. For DTA analysis sample, the heat flows were monitored and recorded by a PC connected with the DTG-60 apparatus, in order to evaluate glass transition temperature, enthalpy, and melting temperature of analyzed samples. The experiments were performed in triplicate and showed good reproducibility.

Thickness

Thickness of the film was determined using the Sample Thickness Tester DM-G, consisting of a digital indicator (Digital Dial Indicator), connected to a PC. All the experimental results are shown both in digital form on a display than graphically to the computer. Once planted the tool on the film, the reading is made twice per second (the tool automatically performs three readings, minimum value that cannot be changed), measuring a minimum, maximum, and average value of a series of measures. The thickness value is expressed in μm or inches and the measuring range is from 12.5 μm to 100 μm, with a resolution of 0.001 μm. The reported results are an average of 30 experimental tests run at 30 different points on the polymer film surface, at room temperature. Measurements were performed at least in triplicate and the mean value thickness is presented.

IR spectroscopy

The FTIR spectra were recorded for commercial and surface-modified PLA sample films by a Perkin-Elmer-1725-X spectrophotometer. They were recorded from 4000 cm^{-1} to 400 cm^{-1} with a resolution of 2.0 cm^{-1}. The results are an average of three experimental tests run on three different samples for each PLA film, to test the results reproducibility. The tests were performed at room temperature, directly on the film, without any preliminary treatments.

Carbon dioxide and oxygen transmission rate

Gas permeability of the films were determined with GDP-C Brugger Feinmechanik GmbH permeability device, a manometric method model, according to ISO 15 105-1 and ASTM D1434, Standard test Method for Determining Gas Permeability Characteristics of Plastic Film and Sheeting and to Gas Permeability Testing Manual, Registergericht München HRB 77020, Brugger Feinmechanik GmbH. The equipment consists of two chambers between which the film is placed. The chamber on the film is filled with the gas used in the test (CO_2 or O_2), at a pressure of 1 atm. A pressure transducer, set in the chamber below the film, records the increasing of gas pressure, P, as a function of the time, t. From pressure/time plot the software automatically calculates permeation, which can be converted in permeability knowing the film thickness.

The film sample of approximately 12 cm × 12 cm in size was placed between the top and the bottom of the permeation cell. The gas transmission rate (GTR), i.e., the value of the film permeability to gas, expressed in $cm^3\ m^{-2}\ d^{-1}\ bar^{-1}$, was determined considering the increase in pressure in relation to the time and the volume of the device. The increase in pressure during the test was calculated and showed using an external PC connected to the instrument, reporting on the x-axis the time in minutes while on the y-axis the GTR value. In order to calculate the GTR value on the y-axis was reported the dP value (hPa) while on the x-axis was reported the time (min). The y-representation is in logarithmic form (250 hPa min^{-1}).

The operative conditions are: room condition of 23°C, with a relative humidity of 26%; gas stream of 100 $cm^3\ min^{-1}$, 0% of gas relative humidity; sample area of 78.4 cm^2.

Films were analyzed at a temperature of 23°C (standard temperature analysis) and of 7°C (simulated condition of fresh cut vegetable food storage temperature), using as test gas analysis 100% O_2 and 100% of CO_2. The gases used in the measure are dry, 0% RH (relative humidity). In the GTR value reported in literature, the term d (which is related to day) is often replaced with 24 h (which is related to 24 h). Permeability measurements were performed at least in triplicate and the mean value is presented. The Method A was used for the analysis, as just reported in the literature,[12–14] with evacuation of top/bottom chambers.

Temperature analysis was set by using an external thermostat HAAKE-Circulator DC10-K15 type.

A gas mixing system Witt-Gasetechnik GmBh & Co KG (Germany) type Km 100-4 was used to obtain the gas flow inside the permeability device.

Statistical analysis

One-way analysis of variance (ANOVA) and test of mean comparisons according to Fisher's least

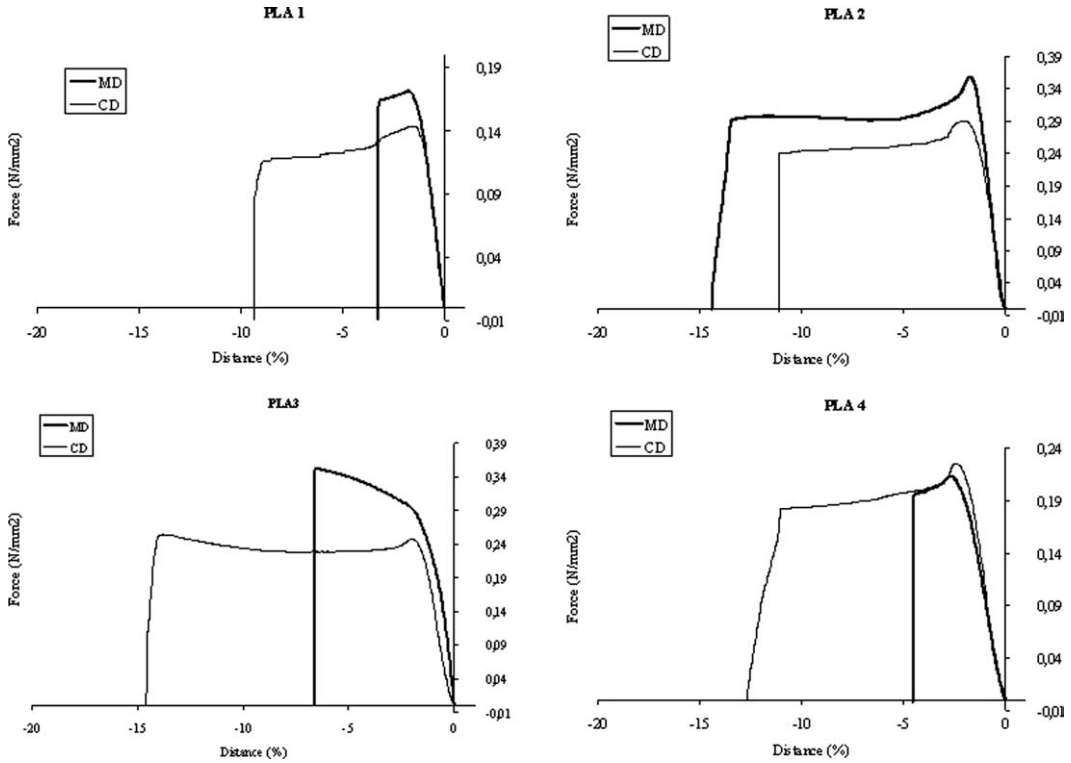

Figure 2 Stress–strain curves (N mm^{-2} %) for PLA 1–4 films in MD and CD extrusion direction.

significant differences (LSDs) were applied on the obtained results, with a level of significance of 0.05. The statistical package STS Statistica for Windows, version 6.0 (Statsoft Inc., Tulsa, OK) was used.

RESULTS AND DISCUSSION

Mechanical properties

Tensile test results, both in the MD and CD directions, are presented. It is important to notice that during mechanical tests many samples do not show break, also during prolonged strain. It means that films under investigation are not homogeneous, with repercussion on the mechanical behavior.

Figure 2 shows the stress–strain curves obtained for PLA 1–4 films. For PLA 1, it can be seen how the curves in the two different directions are totally different, with a different mechanical behavior, characterized by a similar tensile strength of 0.172 and 0.144 N mm^{-2} respectively, but with a different elongation at break of 0.773 and 7.362%, respectively. Also the tenacity is different for the two different film direction, 0.2158 and 0.1365 N mm^{-2} % respectively, which means that the MD film is 37% more toughness than the CD film. Greater is the toughness value, greater must be the energy required to break the sample. So the MD sample, dissipating energy, is therefore more resistant. This parameter is particularly important from a technological point of view because it provides further guidance on the processing and use of film direction to avoid breakage during physical and mechanical manipulations (machine food enveloping and thermal sealability).

For PLA 2 film, in MD and CD direction, it can be noticed elongation and breaking. The MD sample shows a little bit greater value of tensile strength (0.359 N mm^{-2}) compared to the CD sample (0.290 N mm^{-2}), of approximately 20%, but a different elongation at break of 11.589 and 9.016%, respectively, and a tenacity value practically comparable of 0.3468 and 0.3638 N mm^{-2} % for CD and MD sample. This film shows a more homogeneity on the mechanical performance, in both directions.

For PLA 3 film, in MD and CD direction, elongation and breaking is recorded. In this case, the MD sample shows a 30% greater value of tensile strength (0.352 N mm^{-2}) compared to the sample cut into the CD direction (0.248 N mm^{-2}), with a less value of percentage of elongation of 6.566 and 11.911%, respectively, and a tenacity of 1.86 and 0.2658 N mm^{-2} %, respectively, which means that the MD film is 86% more toughness than the CD film. Also in this case the MD sample shows better mechanical properties, as tenacity and toughness.

For PLA 4 film, the CD sample presents a greater value of tensile strength (0.225 N mm^{-2}) compared to the MD sample (0.213 N mm^{-2}), of around 5%, with a value of percentage of elongation significantly

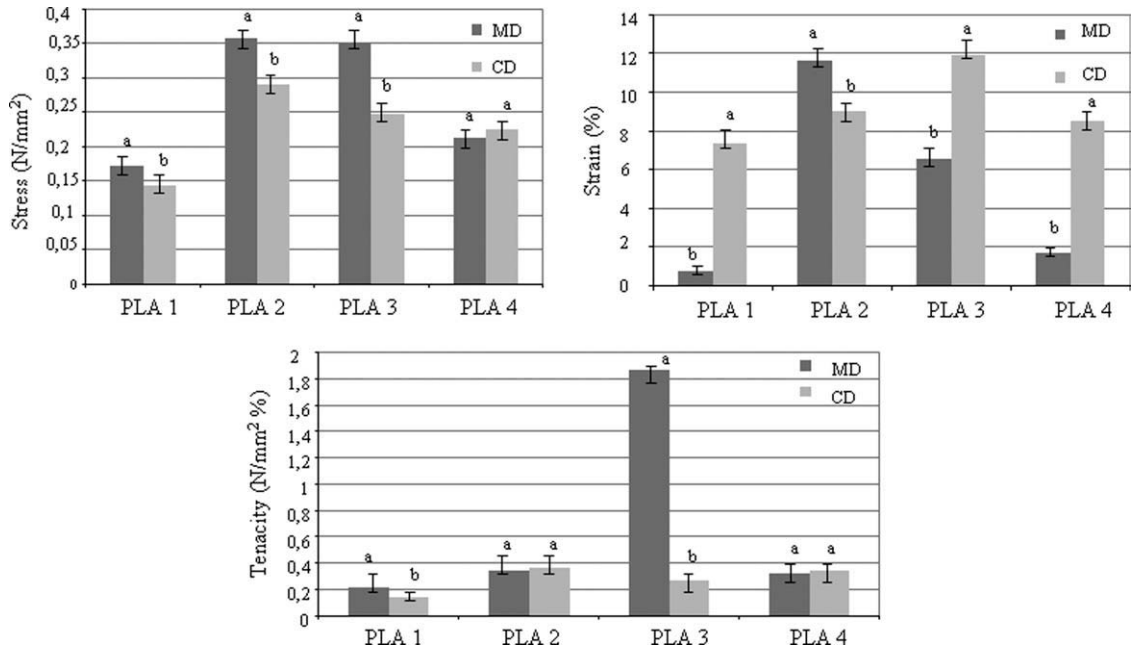

Figure 3 Tensile stress value (stress N mm^{-2}), fracture elongation (strain %), and tenacity (N mm^{-2} %) for PLA sample films, in MD and CD extrusion direction. Values for the same sample with different letter are significantly different ($P < 0.05$).

higher, 8.536% against 1.692%. The toughness for the MD sample was slightly higher than for the CD sample, 0.3437 against 0.3185 N mm^{-2} %, respectively.

The histograms reported in Figure 3 show that PLA films are anisotropic, i.e., showing a different mechanical behavior depending on the orientation (MD and CD) during the tensile test. Stress–strain behavior shows that the percentage of elongation is greater in the CD direction for samples PLA 1, PLA 3, and PLA 4, while for the PLA 2 sample the percentage of elongation is greater in the MD than CD direction. Overall, the more resistant samples were PLA 2 and PLA 3 films in the MD direction and the most tenacious was the PLA 3 sample, always in the MD direction.

Comparing the data obtained with those known from synthetic polymer materials (as LDPE and HDPE) it can be seen how the mechanical properties of polymeric PLA films are generally worse, which makes these materials more suitable to applications requiring no high strength of the film.[15] The PLA has, however, mechanical properties intermediate between those of PET and PS polymers, widely used as food packaging, but easily changes its physical properties and so its mechanical behavior by simply changing its chemical composition (L- and D-isomers quantity) and handling operations.[4]

Physical properties

For that concerns the calorimetric results, it is well-established that the melting behavior of a polymer is affected by its previous thermal history. To provide the same heat treatment to all the samples investigated, samples have been stored at ambient temperature for 30 days. The DSC traces are reported in Figure 4, while in Table I are the reported experimental data:

In all cases, glass transition and melting are evident. It can be seen from the first scan that the PLA film is a multilayer material, showing a first transition phase, represented by two endothermic peaks, corresponding to the fusion of the polymer substrate material on which PLA is added. Different semicrystalline polymers show multiple peaks that may be due to the presence of two or more crystalline groups with different morphology, i.e., crystallites with varying degrees of perfection and/or size. The first two T_m values, represented by endothermic phenomena, are so correlated to the substrate polymer film behavior. Then, another transition phase was recorded, always represented by an endothermic phenomena, corresponding to the PLA film, with a ΔH value which was used to calculate the corresponding PLA crystallinity, determined by the following formula: $x_c = 100\ (\Delta H_m/\Delta H_m^c)$, where ΔH_m is the fusion enthalpy calculated from the experimental curve while $\Delta H_m^c = 93$ J g^{-1} is the fusion enthalpy for the pure crystalline PLA.[16] From the second scan was recorded the T_g value, with the corresponding Δc_p value, and a small endothermic peak corresponding to a residual crystalline PLA, with a T_m value slightly higher due to a more perfect crystallites. From the data reported in Table I, it

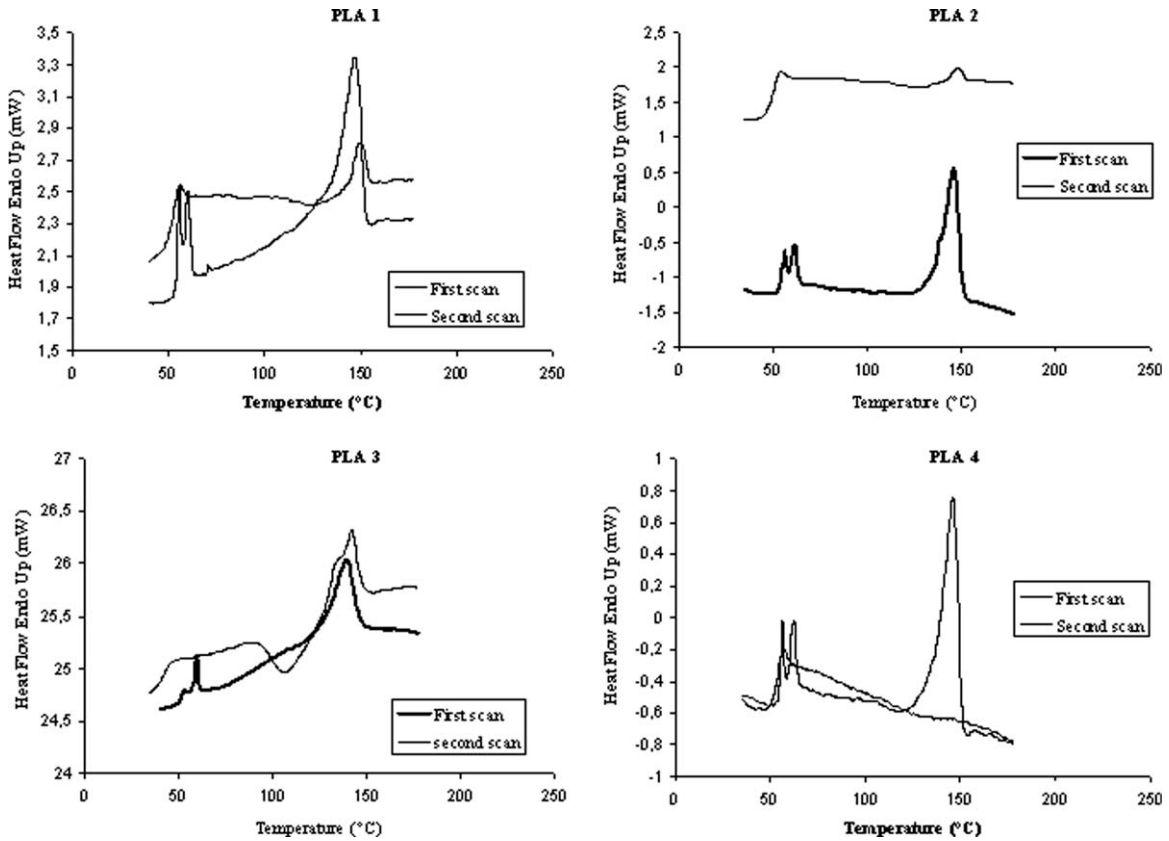

Figure 4 Calorimetric curves of PLA 1–4 films, –first and . . .second scan at 10°C min^{-1}.

can be seen that the recorded melting temperatures are slightly different for the four films due to the non-homogeneity of the films, which confirm that small chemical difference involves small differences in thermal and mechanical behavior. It must be also considered that additives like plasticizers, charged, residual solvents can affect the material final properties.

The PLA behavior as T_m, T_g, crystallinity, and mechanical strength strongly depend on its molecular architecture. Even, as for other polymeric materials, final properties of the PLA depend also from the process conditions adopted (e.g., temperature of extrusion and/or molding). Further, changing the amount of D- or L-isomer during the synthesis of the PLA polymer can be achieved or a totally amorphous polymer or a polymer with percentage of crystallinity exceeding 40%. The crystallinity percentage greatly enhanced the mechanical properties of material giving a PLA with a wide range of values of hardness and rigidity. Crystallinity affects also the T_g value, which may vary from 50 to 80°C, and the melting temperature which can go from 130 to 180°C value.[16] Also, a totally crystalline PLA requires months if not years to be completely degraded to lactic acid. Samples examined in this work shows crystallinity percentage change, from pure PLA sample to the surface-modified samples, probably due to the different superficial treatments used to change permeation properties.

TABLE I
Glass Transition Temperatures (T_g), Onset Melting Temperatures (T_o), Peak Melting Temperatures (T_m) for PLA Films in Static air Atmosphere and in Flowing Nitrogen at 10 °C min^{-1}

		Air static atmosphere			Nitrogen flow		
Films	x_c	T_g (°C)	T_o (°C)	T_m (°C)	T_g (°C)	T_o (°C)	T_m (°C)
PLA 1	22.6	59.7	143.6	149.8	59.7	141.7	150.9
PLA 2	17.9	59.4	135.9	149.8	60.3	137.8	151.2
PLA 3	7.6	59.8[a]	142.8	147.3	58.7[a]	143.8	148.3
PLA 4	19.7	59.1	142.7	148.9	57.8	139.1	150.2

[a] From second scan.

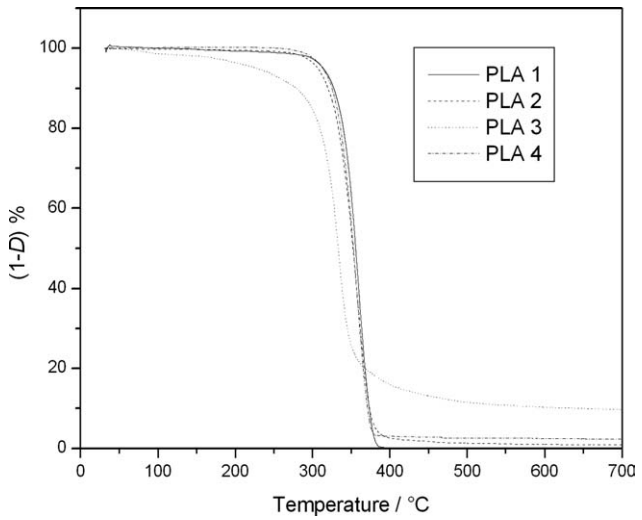

Figure 5 TG curves under N_2 flow of PLA films at the heating rate of 10°C min^{-1}.

Concerning the TG and DTA, experiments were carried out in the scanning mode, in both flowing nitrogen and in a static air atmosphere, but the thermal behavior in the two investigated environments was substantially the same for each PLA film. In the scanned temperature range (35–700°C), all films degraded through a single stage without formation of appreciable residue. The TG curves at 10°C min^{-1} in both inert and oxidative atmospheres are reported in Figures 5 and 6, respectively.

Since the thermal stability of polymers is connected with both initial decomposition temperature and degradation rate,[17] the data of the temperature at the maximum rate of weight loss (T_{max}) as well as the initial decomposition temperatures (T_i) of our polymers are considered and reported in Table II. The onset initial decomposition temperatures at the various heating rates were obtained by the TG curves as the intersection between the starting mass line and the maximum gradient tangent to the TG curve.[18–22]

TABLE II
Initial Decomposition Temperatures (T_i) and Temperatures at Maximum Rate of Weight Loss (T_{max}) for PLA Films in Static Air Atmosphere and in Flowing Nitrogen at 10 °C min^{-1}

	Air static atmosphere		Nitrogen flow	
Films	T_i (°C)	T_{max} (°C)	T_i (°C)	T_{max} (°C)
PLA 1	330.7	361.8	332.9	364.5
PLA 2	333.6	359.3	327.2	361.7
PLA 3	306.9	338.6	307.7	334.8
PLA 4	334.8	365.0	332.8	360.1

The obtained results suggest some considerations. The thermal behavior, inert or oxidative degradation, of the investigated PLA films appears not influenced by the environment. Moreover, not only the shape of the TG curves in the two used experimental conditions is very similar but, also, the initial decomposition temperatures under nitrogen flow are very close to those in static air atmosphere (Table II), suggesting that the presence of oxygen does not influence the initial mechanism of decomposition. The T_i as well as the T_{max} of PLA 1, 2, and 4 are largely higher, about 25–30°C than that of the corresponding anti-UV coating PLA films, indicating lower thermal stability of PLA 3 in respect to the other PLA films, being T_i a determining parameter on the thermal stability of polymers.[20]

For semicrystalline PLA, both the melting temperature (T_m) and glass transition temperature (T_g) are important physical parameters for predicting PLA behavior, in particular a qualitative and quantitative

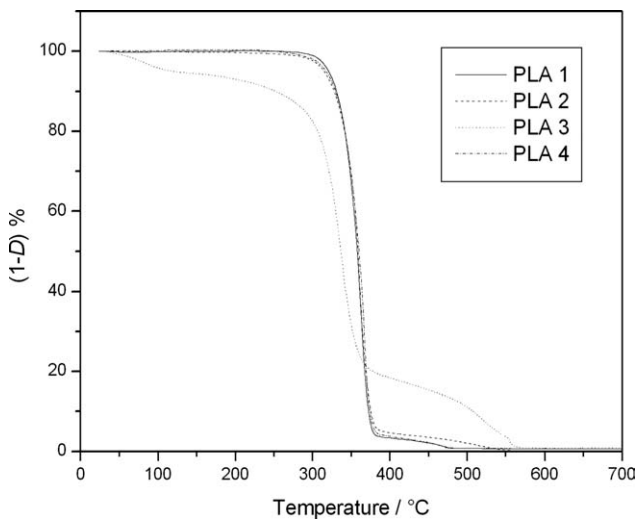

Figure 6 TG curves in static air atmosphere of PLA films at the heating rate of 10°C min^{-1}.

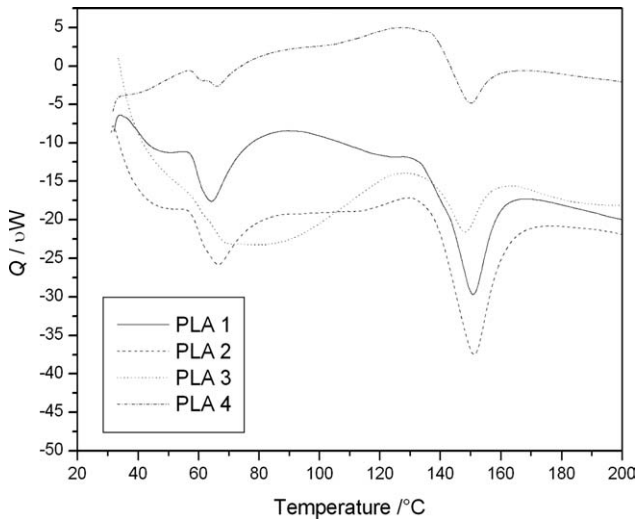

Figure 7 DTA curves under N_2 flow of PLA films at the heating rate of 10°C min^{-1}.

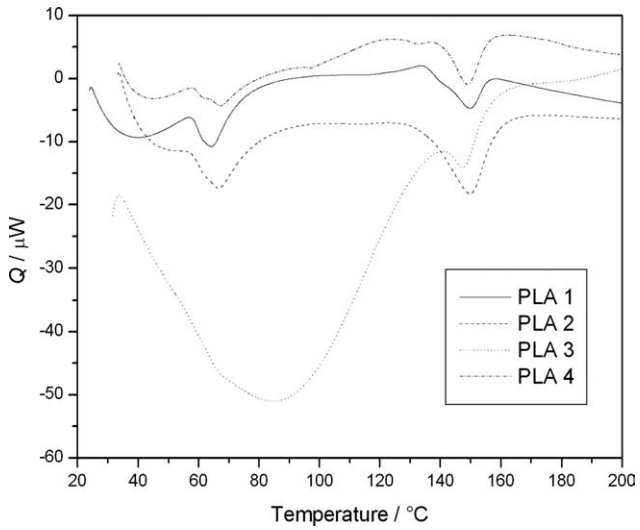

Figure 8 DTA curves in static air atmosphere of PLA films at the heating rate of 10°C min^{-1}.

understanding of the transition temperatures as well as other polymer properties is important to identify polymer applications.[23] It is well known that service temperature of semicrystalline PLA is not far beyond T_g.[23,24]

Results from DTA analysis, in both flowing nitrogen and in a static air atmosphere, were reported in Table II and are in agreement with those reported in the literature, where the typical PLA glass transition temperature range is reported.[23–25]

As shown in Figures 7 and 8, DTA curves of PLA 3 in both flowing nitrogen and in the static air atmosphere are different from each other showing an endothermic event superimposed on T_g. Probably this endothermic relaxation is due to a secondary molecular reordering in the amorphous phase of the semicrystalline polymers, and should disappear if the sample will be heated above T_g.[23]

In order to confirm this hypothesis, additional DTA scans were carried out for PLA 3, the first one up to 120°C and the second one above the melting temperature. As shown in Figure 9 in the second DTA scan, the endothermic relaxation disappears and it was possible to detect the glass transition temperature.

This different thermal behavior of PLA 3 can be attributed to a decrease in density and crystallinity (Table I)[26] and have shown that exposure to UV causes a decrease in density of about 20 kg m^{-3} and a decrease in crystallinity of about 12%, furthermore have demonstrated as an increase or decrease of the initial decomposition temperature is related to the increase or decrease of polymer density.[20]

Infrared Analysis

FTIR spectra were recorded for each sample in order to investigate the chemical structure. The principle PLA 1, 2, and 4 absorption bands in the infrared range are summarized in Table III. The IR bands at 2997 cm^{-1} and 2946 cm^{-1} are assigned to the CH stretching region, $\nu_{as}CH_3$ and ν_sCH_3 modes. The C=O stretching region is observed as a band at 1747 cm^{-1}. The region between 1500 cm^{-1} and 1360 cm^{-1} is characterized by the 1452 cm^{-1} CH_3 band. The CH deformation and asymmetric bands appear at 1380 cm^{-1} and 1360 cm^{-1}, respectively. In the region of 1300 cm^{-1} to 1000 cm^{-1}, it is possible to observe the C—O stretching modes of the ester groups at 1267 cm^{-1} and the νO—C asymmetric mode at 1180 cm^{-1}. Between 1000 cm^{-1} and 800 cm^{-1}, peaks can be observed at 956 cm^{-1} and 921 cm^{-1} which can be attributed to the characteristic vibrations of the helical backbone with CH_3 rocking modes. Two bands related to the crystalline and amorphous phases of PLA were found at 868 cm^{-1} and 756 cm^{-1}. The peak at 868 cm^{-1} can be assigned to the amorphous

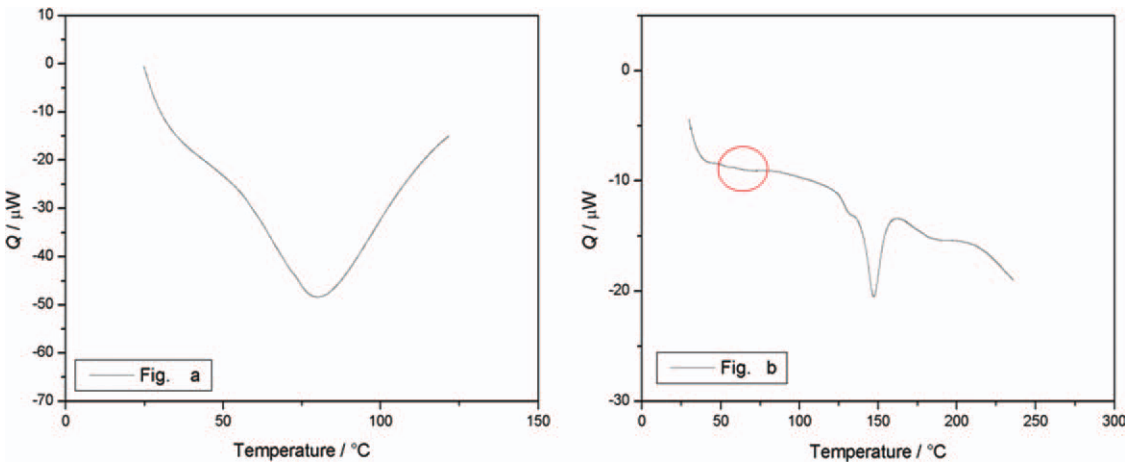

Figure 9 DTA of PLA 3 film (a) up to 120°C and (b) above the melting temperature at the heating rate of 10°C min^{-1}. [Color figure can be viewed in the online issue, which is available at wileyonlinelibrary.com.]

TABLE III
Infrared Spectroscopy Data—Peak Band Assignments for PLA 1, 2, and 4 Infrared Spectra

Assignment	Peak position (cm^{-1})
—OH stretch (free)	3570
—CH— stretch	2997 (asym), 2946 (sym)
—C=O carbonyl stretch	1747
—CH_3 bend	1452
—CH— deformation symmetric and asymmetric bend	1380, 1360
—C=O bend	1267
—C—O— stretch	1180, 1127, 1083
—OH bend	1043
—CH_3 rocking modes	956, 921
—C—C— stretch	922, 868

phase and the peak at 756 cm^{-1} to the crystalline phase. Similar findings have been reported in the literature.[23,27]

For the PLA 3 sample, the absorption band are different, due to an initial degradation of the samples, as can be see from the Figure 10, where the FTIR spectra of PLA films are shown.

Barrier Properties

The barrier behavior of the package system depends upon the product's characteristics and intended end-use application. Carbon dioxide and oxygen are two of the main permeants studied in packaging applications, especially in modified-atmosphere packaging application (MAP technique), because they may transfer from internal or external environment through the polymer package wall, influencing continuously the product quality and shelf-life. Therefore, to study the gas permeability of a polymer is crucial to understand and estimate its utility for the product-package shelf-life.

Permeability measures were carried out on the PLA films and the GTR value are reported in Table IV.

The GTR data, at a given temperature set test, are recorded and graphically represented with the GTR values on the *y*-axis while in the *x*-axis is reported the time-test in hours or minutes. The test can be stopped when the representative curve is in its equilibrium state or when the permeate concentration (or gas pressure) value is constant for a period of time relatively long.

The GTR value and any other permeability parameters are obtained by the curves, reporting the pressure difference between the two cells, in logarithmic form, in function of the time ($dP\ t^{-1}$).

Temperature has a big influence on the transmission of the gas through the material. The mechanisms that drive the adsorption/desorption permeability, solubility, and diffusion phenomena are all closely dependent to the temperature. Relations that bind the diffusion coefficients (*D*) and solubility (*S*) with temperature are of exponential nature and follow the Arrhenius law. Measures to study the permeability of packaging material are conducted under standardized temperatures (23 and 38°C) which are usually different from the end use temperature. Knowledge about the behavior of materials at different temperatures is therefore essential to adopt the best food packaging solution, especially for food products destined to a refrigerated distribution. Permeability

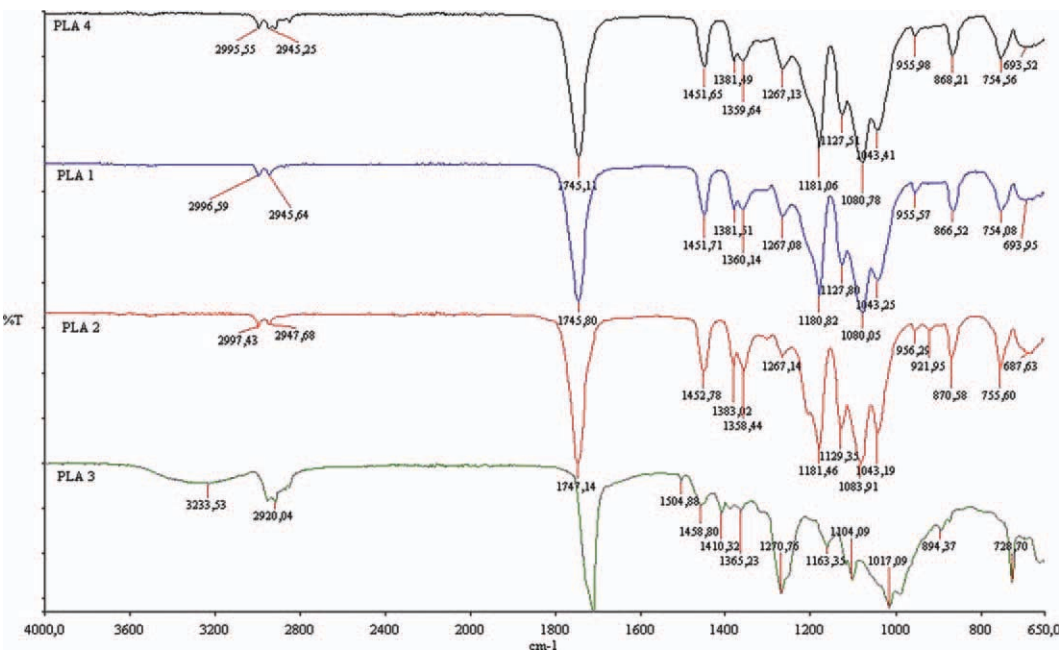

Figure 10 FTIR spectra of PLA films. [Color figure can be viewed in the online issue, which is available at wileyonlinelibrary.com.]

TABLE IV
PLAs Permeability Parameters

Sample	Thick (μm)	CO_2		O_2	
		GTR (7°C)	GTR (23°C)	GTR (7°C)	GTR (23°C)
PLA 1	27	775.67 ± 3.40 (a)	1201.00 ± 1.73 (b)	301.33 ± 3.51 (a)	487.67 ± 2.52 (b)
PLA 2	41	3.17 ± 0.21 (a)	10.57 ± 0.15 (b)	2.07 ± 0.06 (a)	5.37 ± 0.09 (b)
PLA 3	44	2.48 ± 0.02 (a)	5.13 ± 0.15 (b)	1.89 ± 0.02 (a)	4.43 ± 0.01 (b)
PLA 4	30	3.07 ± 0.12 (a)	9.90 ± 0.20	6.80 ± 0.30 (a)	12.83 ± 0.06 (b)

measures shows as all PLA samples have a gas permeability value higher at 23°C than at 7°C.

For PLA 1 sample, ranging from 23 to 7°C, the CO_2 permeability shows a decrease of 35%, having an average value respectively equal to 1201 $cm^3\ m^{-2}\ d^{-1}\ bar^{-1}$ at 23°C and 775.67 $cm^3\ m^{-2}\ d^{-1}\ bar^{-1}$ at 7°C. The O_2 permeability value shows a decrease of 38% from 23 to 7° C, exactly going from a GTR value of 487.67 to a value of 301.33 ($cm^3\ m^{-2}\ d^{-1}\ bar^{-1}$). Following permeability values recorded to oxygen and carbon dioxide, the PLA 1 film can be defined as a film with medium permeability.

As reported in Table IV, CO_2 and O_2 permeability data for the PLA 2, 3, and 4 films have been far lower than those obtained for the PLA 1 sample. For PLA 2, ranging from 23 to 7°C, the CO_2 permeability shows a decrease of 70%, having an average value, respectively, equal to 10.57 $cm^3\ m^{-2}\ d^{-1}\ bar^{-1}$ at 23°C and 3.17 $cm^3\ m^{-2}\ d^{-1}\ bar^{-1}$ at 7°C. The O_2 permeability value shows a decrease of 61% from 23 to 7°C, exactly going from a GTR value of 5.37 $cm^3\ m^{-2}\ d^{-1}\ bar^{-1}$ to a value of 2.1 $cm^3\ m^{-2}\ d^{-1}\ bar^{-1}$. For PLA 3, ranging from 23 to 7°C, the CO_2 shows a permeability decrease of 51%, having an average value, respectively, equal to 5.13 $cm^3\ m^{-2}\ d^{-1}\ bar^{-1}$ at 23°C and 2.48 $cm^3\ m^{-2}\ d^{-1}\ bar^{-1}$ at 7°C. The O_2 permeability value shows a decrease of 57% from 23 to 7°C, exactly going from a GTR value of 4.43 $cm^3\ m^{-2}\ d^{-1}\ bar^{-1}$ to a value of 1.89 $cm^3\ m^{-2}\ d^{-1}\ bar^{-1}$. For PLA 4, ranging from 23 to 7°C, the CO_2 permeability shows a decrease of 69%, having an average value, respectively, equal to 9.9 $cm^3\ m^{-2}\ d^{-1}\ bar^{-1}$ at 23°C and 3.07 $cm^3\ m^{-2}\ d^{-1}\ bar^{-1}$ at 7°C. The O_2 permeability value shows a decrease of 47% from 23 to 7°C, exactly going from a GTR value of 12.83 $cm^3\ m^{-2}\ d^{-1}\ bar^{-1}$ to a value of 6.8 $cm^3\ m^{-2}\ d^{-1}\ bar^{-1}$.

It can be noticed as the GTR value of PLA 2, 3, and 4 films are reduced by more than two orders of magnitude after addition of the coating surface (UV additives, SiO_x, and varnish). These films are therefore far less permeable to both tested gases and could be defined as high-barrier films that could be used for those foods where the presence of O_2 must be completely or almost completely avoided, such as fat product, cheese, and fresh cut food, to eliminate and/or reduce oxidative degradation processes.

Regarding the type of gas, although molecular size of permeating species could affect the transmission speed, for gases utilized on food packaging application (such as O_2, CO_2, and N_2) there is no relationship between molecular size and permeability behavior. For polymer material CO_2 is more permeable with respect to the other gases, although its molecular diameter (3.4 Å) is greater than that of the O_2 (3.1 Å) and N_2 (3.0 Å). Permeability ratio (also called selectivity) of these gases is fairly constant for all polymers used in food packaging application. As reported in the literature,[28] such data are very useful because they give the possibility to determine the unknown gas permeability knowing the gas permeability of another gas. Therefore it would be enough simply measuring the value of, for example, CO_2 permeability to derive the value of the O_2 permeability simply dividing the result obtained for the relative ratio. In reality, the relationship between the two gas permeability data is not applicable to all polymeric materials and not all show the same value of selectivity ratio. For example, Auras et al.[16] reported that the O_2 permeability values are lower around 10 orders of magnitude than the CO_2 permeability values. Therefore, the simple statement that permeability values are constants for all polymers is not always true. It would cause serious errors to consider constants such parameters and use them to predict values of permeability of any material, as reported also by Guisheng et al.,[29] which checked

TABLE V
(CO_2 and O_2) GTR Average Value at 23 and 7°C Versus Selectivity Ratio

Sample	GTR CO_2 (23°C/7°C)	GTR O_2 (23°C/7°C)	Selectivity ratio
PLA 1	1201.00/775.67	487.67/301.33	2.46/2.57
PLA 2	10.57/3.17	5.37/2.07	1.97/1.52
PLA 3	5.13 / 2.48	4.43/1.89	1.16/1.31
PLA 4	9.90/3.07	12.83/6.80	0.77/0.45

the relationship between the permeability for two gases, CO_2 and O_2, through a series of different polymers used in packaging applications. As reported in Table V, this assumption was demonstrated also from our experimental data, with different selectivity ratios for CO_2 and O_2, respectively, at 23°C and 7°C for PLA samples. Our results confirm that for PLA1, 2, and 3 films, the CO_2 permeability value is greater than that of O_2 value, but in different amount depending on the analyzed film and experimental temperature, but for PLA 4 film the O_2 GTR value is greater than the CO_2 GTR value, confirming that the film barrier behavior depends on the material structure.

CONCLUSIONS

PLA is a polymer material with potential applications in the field of food packaging but this study demonstrated that those films behavior could be affected by the treatment, depending on the chemical structure of the film and of the processing condition.

Comparing the mechanical data obtained with those known from synthetic polymer materials (HDPE, LDPE) it can be seen how the PLA films properties are generally worse, which makes these materials more suitable for applications which require no high strength of the film. But PLA has, however, mechanical properties intermediate between those of PET and PS polymers also widely used as food packaging. All PLA films show a lower T_m and T_g value than, for example, PET and PS, which make PLA more suitable for heat sealing and thermal processing. Further, from the thermogravimetric analysis, polymers tested showed great structural stability.

Permeability of plastic packaging is of scientific and technical importance, especially in relation to the development and introduction of new packaging material. Concerning the barrier properties, natural PLA showed that CO_2 and O_2 permeability coefficients are lower than the synthetic polymer, while for the PLA-coated film the coefficients value are very different, changing drastically from a low to a very high barrier material.

However it seems that is not possible to have a PLA film adequate for all food packaging system but it is necessary to study a PLA material for each application. Maybe, until now, the best biodegradable food packaging material is a combination of PLA with a synthetic polymer, in different percentage, which could potentially provide the best market solution. Many different materials are present on the market but, of course, further research should be carried out on PLA film in real life environmental conditions, to examine the interaction between the food product and the packaging material. In particular, the effect of storage conditions (time, temperature, relative humidity, and contact with different kind of foods) on the mechanical and physical properties has to be evaluated. Further, is important to know how the material reacts under different conditions like heating or sterilization and freezing, because these are the treatments (like exposure to the radiation in the microwave oven or freezing in the deep freezer) for preservation that may be used in a household.

References

1. www.european-bioplastics.org
2. Kirwan, M. J.; Strawbridge, J. W. Food Pack Technol 2003, 174.
3. Arvanitoyannis, I. S. J Macromol Sci Rev Macromol Chem Phys 1999, C39(2), 205.
4. Auras, R.; Singh, S. P.; Singh, J. J. Pack Technol Sci 2005, 18, 207.
5. Grüniger, A.; Rudolf von Rohr, Ph. Thin Solid Films 2004, 459, 308.
6. Hedenqvist, M. S.; Johansson, K. S. Surf Coat Technol 2003, 172, 7.
7. Galić, K.; Ciković, N. Food Technol Biotechnol 2003, 41, 247.
8. Galotto, M. J.; Ulloa, P. A.; Hernández, D.; Fernández-Martín, F.; Gavara, R.; Guarda, A. Pack Technol Sci 2008, 21, 297.
9. Siracusa, V.; Rocculi, P.; Romani, S.; Dalla Rosa, M. T. Food Sci Technol 2008, 19, 634.
10. Conn, R. E.; Kolstad, J. J.; Borzelleca, J. F.; Dixler, D. S.; Filer, L. J., Jr.; LaDau, B. N.; Pariza, M. W. Food Chem Toxicol 1995, 33, 273.
11. Shimadzu DTG-60/60H Instruction Manual; Shimadzu Corporation, Analytical & Measuring Instruments Division: Kyoto, Japan, 2000.
12. Gajdoš, J.; Galić, K.; Kurtanjek, Ž.; Ciković, N. Polym Test 2000, 20, 49.
13. Mrkić, S.; Galić, K.; Ivanković, M.; Hamin, S.; Ciković, N. J Appl Polym Sci 2006, 99, 1590.
14. Gas Permeability Testing Manual, Registergericht München HRB 77020, Brugger Feinmechanik GmbH, 2008.
15. Petersen, K.; Nielsen, P. V.; Olsen, M. B. Starch/Staerke 2001, 53, 356.
16. Auras, R.; Harte, B.; Selke, S.; Hernandez, R. J Plast Film Sheet 2003, 19, 123.
17. Blanco, I.; Abate, L; Antonelli, M. L. Polym Degrad Stab 2011, 96, 1947.
18. Abate, L.; Blanco, I.; Cicala, G.; La Spina, R.; Restuccia, C. L. Polym Degrad Stab 2006, 91, 924.
19. Abate, L.; Blanco, I.; Cicala, G.; Recca, G.; Scamporrino, A. Polym Eng Sci 2009, 49, 1477.
20. Abate, L.; Blanco, I.; Cicala, G.; Mamo, A.; Recca, G.; Scamporrino, A. Polym Degrad Stab 2010, 95, 798.
21. Schmidt, V.; Soldi, V. Polym Degrad Stab 2006, 91, 3124.
22. Causin, V.; Marega, C.; Marigo, A.; Ferrara, G.; Idiyatullina, G.; Fantinel, F. Polymer 2006, 47, 4773.
23. Auras, R.; Harte, B.; Selke, S. Macromol Biosci 2004, 4, 835.
24. Witzke, D. R. Thesis PhD. Michigan State University, East Lansing, MI, 1997; p 389.
25. Ikada, Y.; Tsuji, H. Macromol Rapid Commun 2000, 21, 117.
26. Hoekstra, H. D.; Spoormaker, J. L.; Breen, J.; Audouin, L.; Verdu, J. Polym Degrad Stab 1995, 49, 251.
27. Garlotta, D. J Polym Environ 2002, 9, 63.
28. Van Krevelen, D. W. Polymer Properties, 3rd completely revised edition; Elsevier: Amsterdam, 1997; 898 p.
29. Guisheng, F.; Incarnato, L.; Di Maio, L.; Acierno, D. Polymer 1995, 36, 4345.